

Redox-Switched Complexation/Decomplexation of K^+ and Cs^+ by Molecular Cyanometalate Boxes

Julie L. Boyer, Maya Ramesh, Haijun Yao, Thomas B. Rauchfuss,* and Scott R. Wilson

Contribution from the Department of Chemistry, University of Illinois at Urbana–Champaign, Urbana, Illinois 61801

Received June 30, 2006; E-mail: rauchfuz@uiuc.edu

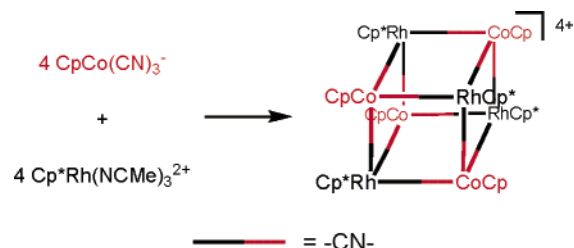
Abstract: The reaction of $[N(PPH_3)_2][CpCo(CN)_3]$ and $[Cb^*Co(NCMe)_3]PF_6$ ($Cb^* = C_4Me_4$) in the presence of K^+ afforded $\{K[CpCo(CN)_3]_4[Cb^*Co]_4\}PF_6$, $[KCo_8]PF_6$. IR, NMR, ESI-MS indicate that $[KCo_8]PF_6$ is a high-symmetry molecular box containing a potassium ion at its interior. The analogous heterometallic cage $\{K[Cp^*Rh(CN)_3]_4[Cb^*Co]_4\}PF_6$ ($[KRh_4Co_4]PF_6$) was prepared similarly via the condensation of $K[Cp^*Rh(CN)_3]$ and $[Cb^*Co(NCMe)_3]PF_6$. Crystallographic analysis confirmed the structure of $[KCo_8]PF_6$. The cyanide ligands are ordered, implying that no Co–CN bonds are broken upon cage formation and ion complexation. Eight Co–CN–Co edges of the box bow inward toward the encapsulated K^+ , and the remaining four μ -CN ligands bow outward. MeCN solutions of $[KCo_8]^+$ and $[KRh_4Co_4]^+$ were found to undergo ion exchange with Cs^+ to give $[CsCo_8]^+$ and $[CsRh_4Co_4]^+$, both in quantitative yields. Labeling experiments involving $[(MeC_5H_4)Co(CN)_3]^-$ demonstrated that Cs^+ -for- K^+ ion exchange is accompanied by significant fragmentation. Ion exchange of NH_4^+ with $[KCo_8]^+$ proceeds to completion in THF solution, but in MeCN solution, the exclusive products were $[Cb^*Co(NCMe)_3]PF_6$ and the poorly soluble salt $NH_4CpCo(CN)_3$. The lability of the NH_4^+ -containing cage was also indicated by the rapid exchange of the acidic protons in $[NH_4Co_8]^+$. Oxidation of $[MCo_8]^+$ with 4 equiv of $FcPF_6$ produced paramagnetic ($S = 4/2$) $[Co_8]^{4+}$, releasing Cs^+ or K^+ . The oxidation-induced dissociation of M^+ from the cages is chemically reversed by treatment of $[Co_8]^{4+}$ and $CsOTf$ with 4 equiv of Cp_2Co . Cation recognition by $[Co_8]$ and $[Rh_4Co_4]$ cages was investigated. Electrochemical measurements indicated that $E_{1/2}(Cs^+) - E_{1/2}(K^+) \sim 0.08$ V for $[MCo_8]^+$.

Introduction

Although three-dimensional coordination polymers based on cyanide have been known literally for centuries,^{1,2} the first molecular cyanometalate cage, $[(OC)Pd(CN)Mn(C_5H_4Me)(CO)_2]_4$, was reported only in 1990.³ Since 1998, several cyanometalate cages have been described. Such cages are typically prepared via condensation of facial tricyanometalates, such as $[L_3M(CN)_3]^{z-}$, with facial tritopic Lewis acids (Scheme 1).^{4,5}

Cyanometalate cages adopt diverse structures,^{6–9} but the most prevalent motif is the expanded cube or box comprised of eight

Scheme 1



$M-CN-M'$ linkages with idealized T_d symmetry.^{4,5,10–12} Cyanometalate frameworks have been discussed as components of electronic devices,^{13,14} sensors,¹⁵ molecular magnets,^{16,17} and

- (1) Dunbar, K. R.; Heintz, R. A. *Prog. Inorg. Chem.* **1997**, *45*, 283–391.
- (2) Sharpe, A. G. *The Chemistry of Cyano Complexes of the Transition Metals*; Academic Press: London, 1976.
- (3) Braunstein, P.; Oswald, B.; Tiripicchio, A.; Camellini, M. T. *Angew. Chem., Int. Ed. Engl.* **1990**, *29*, 1140–1143.
- (4) (a) Klausmeyer, K. K.; Rauchfuss, T. B.; Wilson, S. R. *Angew. Chem., Int. Ed.* **1998**, *37*, 1694–1696. (b) Heinrich, J. L.; Berseth, P. A.; Long, J. R. *Chem. Commun.* **1998**, 1231–1232.
- (5) Schelter, E. J.; Prosvirin, A. V.; Reiff, W. M.; Dunbar, K. R. *Angew. Chem., Int. Ed.* **2004**, *43*, 4912–4915.
- (6) (a) Berseth, P. A.; Sokol, J. J.; Shores, M. P.; Heinrich, J. L.; Long, J. R. *J. Am. Chem. Soc.* **2000**, *122*, 9655–9662. (b) Lang, J.-P.; Xu, Q.-F.; Chen, Z.-N.; Abrahams, B. F. *J. Am. Chem. Soc.* **2003**, *125*, 12682–12683. (c) Lee, I. S.; Long, J. R. *Dalton Trans.* **2004**, 3434–3436. (d) Sokol, J. J.; Shores, M. P.; Long, J. R. *Inorg. Chem.* **2002**, *41*, 3052–3054. (e) Sokol, J. J.; Shores, M. P.; Long, J. R. *Angew. Chem., Int. Ed.* **2001**, *40*, 236–239. (f) Contakes, S. M.; Klausmeyer, K. K.; Milberg, R. M.; Wilson, S. R.; Rauchfuss, T. B. *Organometallics* **1998**, *17*, 3633–3635. (g) Kuhlman, M. L.; Yao, H.; Rauchfuss, T. B. *Chem. Commun.* **2004**, 1370–1371. (h) Berlinguette, C. P.; Vaughn, D.; Canada-Vilalta, C.; Galan-Mascaros, J. R.; Dunbar, K. R. *Angew. Chem., Int. Ed.* **2003**, *42*, 1523–1526.

- (7) Contakes, S. M.; Rauchfuss, T. B. *Angew. Chem., Int. Ed.* **2000**, *39*, 1984–1986.
- (8) Contakes, S. M.; Rauchfuss, T. B. *Chem. Commun.* **2001**, 553–554.
- (9) Contakes, S. M.; Kuhlman, M. L.; Ramesh, M.; Wilson, S. R.; Rauchfuss, T. B. *Proc. Natl. Acad. Sci. U.S.A.* **2002**, *99*, 4889–4893.
- (10) Li, D.; Parkin, S.; Wang, G.; Yee, G. T.; Clerac, R.; Wernsdorfer, W.; Holmes, S. M. *J. Am. Chem. Soc.* **2006**, *128*, 4214–4215.
- (11) Klausmeyer, K. K.; Wilson, S. R.; Rauchfuss, T. B. *J. Am. Chem. Soc.* **1999**, *121*, 2705–2711.
- (12) Hsu, S. C. N.; Ramesh, M.; Espenson, J. H.; Rauchfuss, T. B. *Angew. Chem., Int. Ed.* **2003**, *42*, 2663–2666.
- (13) Vahrenkamp, H.; Geiss, A.; Richardson, G. N. *J. Chem. Soc., Dalton Trans.* **1999**, 3643–3651.
- (14) Bignozzi, C. A.; Schoonover, J. R.; Scandola, F. *Prog. Inorg. Chem.* **1997**, *44*, 1–95.
- (15) Beauvais, L. G.; Shores, M. P.; Long, J. R. *J. Am. Chem. Soc.* **2000**, *122*, 2763–2772.
- (16) Beltran, L. M. C.; Long, J. R. *Acc. Chem. Res.* **2005**, *38*, 325–334.

sieves.^{11,12} The rigidity of cyanometalate frameworks should enhance the selectivity of their host–guest behavior. For example, the $\{[\text{CpCo}(\text{CN})_3]_4[\text{Cp}^*\text{Ru}]_4\}$ cage exhibits what appears to be the highest known preference for binding of Cs^+ versus K^+ ($K_{\text{Cs}}/K_{\text{K}} > 10^{12}$).¹² This selectivity is conceptually relevant to the separation of radioactive ^{137}Cs from solutions containing K^+ .¹

The complementation of supramolecular systems with redox behavior is both well established and topical.¹⁸ Incorporation of redox-active components into cyanometalate boxes should allow the host–guest behavior of the box to be modified via changes in the redox poise of the host cage. In previous work on redox-active ion receptors, Plenio described a ferrocene-modified cryptand that exhibits an 80 mV difference when complexed to K^+ versus Cs^+ .¹⁹ The $E_{1/2}$ for a bis(calix[4]-diquinone) sequestrant displays a 60 mV difference for its K^+ versus Cs^+ derivative, although the effect is largely obscured by the multielectron nature of the couple.²⁰ Aside from possible sensor applications, a second motivation for the study of redox-active sequestrants is that their affinities could be switched on and off electrochemically. One would expect that strongly held guests could be decomplexed from hosts by oxidation since cationic frameworks would bind cations more weakly than reduced derivatives. The cyanometalate cages are especially interesting because these structures envelop the guest ion, maximizing the intimacy of the host–guest interaction and, therefore, potentially maximizing the responsiveness of host–guest behavior to the redox state of the cage.

In this report, we describe the use of the $[\text{Cb}^*\text{Co}]^+$ fragment ($\text{Cb}^* = \eta^4\text{-C}_4\text{Me}_4$) for the construction of electro-active cyanometalate cages. The general utility of $[\text{Cb}^*\text{Co}(\text{NCMe})_3]^+$ was established by Herberich,²¹ who prepared this species in good yield starting from 2-butyne and $\text{Co}_2(\text{CO})_8$. Crystallographic studies of $[\text{Cb}^*\text{Co}(\text{NCMe})_3]\text{PF}_6$ showed that the range of N–Co–N bond angles varies from 97.8 to 89.0, which is compatible with box-like cages.

Results and Discussion

Condensation Routes to Co_8 and Co_4Rh_4 Cages. The reaction of equimolar amounts of $[\text{N}(\text{PPh}_3)_2][\text{CpCo}(\text{CN})_3]$ and $[\text{Cb}^*\text{Co}(\text{NCMe})_3]\text{PF}_6$ gave insoluble, apparently nonmolecular products. When, however, the same reaction was conducted in the presence of K^+ , a deep purple solution resulted, from which we could isolate the salt $\{\text{K}[\text{C}[\text{CpCo}(\text{CN})_3]_4[\text{Cb}^*\text{Co}]_4]\text{PF}_6, [\text{KC}_8]\text{PF}_6$. The IR spectrum of this salt featured a band for ν_{CN} at 2147 cm^{-1} versus 2121 cm^{-1} for $[\text{CpCo}(\text{CN})_3]$ in MeCN solution. ESI-MS confirmed the presence of $[\text{KC}_8]^+$ ($m/z = 1515\text{ amu}$). The ^1H NMR spectrum confirmed the high symmetry of $[\text{KC}_8]^+$, with singlets at δ 5.58 (Cp) and 0.96 (Cb*). Solutions of $[\text{KC}_8]^+$ rapidly decompose in air to give an insoluble solid.

The analogous heterometallic $\{\text{K}[\text{C}[\text{Cp}^*\text{Rh}(\text{CN})_3]_4[\text{Cb}^*\text{Co}]_4]\text{PF}_6$ ($[\text{KRh}_4\text{Co}_4]\text{PF}_6$) cage was prepared via the condensation

Table 1. Selected Bond Distances (Å) and Angles (deg) for $\{\text{K}[\text{C}[\text{CpCo}(\text{CN})_3]_4[\text{Cb}^*\text{Co}]_4]\text{PF}_6$

Co1–C1	1.8663(0.0035)	C1–Co1–C2	92.40(0.15)
Co1–C2	1.8566(0.0040)	C1–Co1–C3	84.15(0.15)
Co1–C3	1.8787(0.0036)	C2–Co1–C3	93.11(0.15)
Co2–N1	1.9607(0.0028)	N1–Co2–N2	90.36(0.12)
Co2–N2	1.9613(0.0032)	N1–Co2–N3	95.85(0.12)
Co3–N3	1.9679(0.0028)	N2–Co2–N3	90.35(0.11)
K–C1	3.5326(0.0039)	Co1–C1≡N1	172.73(0.32)
K–C2	3.8406(0.0039)	Co1–C2≡N2	176.97(0.30)
K–C3	3.4559(0.0039)	Co1–C3≡N3	174.13(0.31)
K–N1	3.3825(0.0032)	Co2–N1≡C1	171.32(0.27)
K–N2	3.8947(0.0034)	Co2–N2≡C2	163.02(0.27)
K–N3	3.3025(0.0032)	Co2–N3≡C3	170.23(0.28)

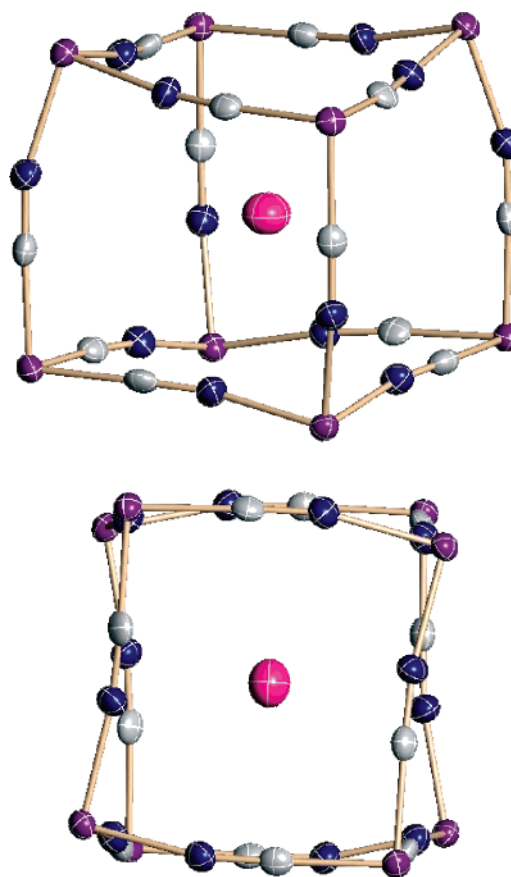


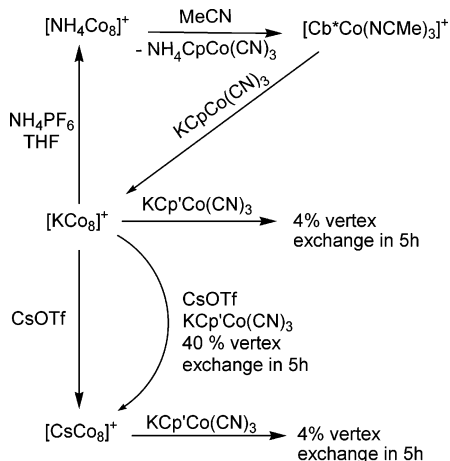
Figure 1. The molecular structure of the metal cyanide core of $\{\text{K}[\text{C}[\text{CpCo}(\text{CN})_3]_4[\text{Cb}^*\text{Co}]_4]\text{PF}_6$ with the Cp and Cb* ligands omitted for clarity. Thermal ellipsoids are drawn at the 50% level. N = blue, C = gray, Co = purple, K = pink.

of $[\text{K}[\text{Cp}^*\text{Rh}(\text{CN})_3]$ and $[\text{Cb}^*\text{Co}(\text{NCMe})_3]\text{PF}_6$. The formation of $[\text{KRh}_4\text{Co}_4]^+$ was confirmed by ^1H NMR and IR spectroscopies as well as ESI-MS. The IR spectrum of this salt featured a single ν_{CN} band at 2146 cm^{-1} , and the ^1H NMR spectrum confirmed the high symmetry.

Crystallographic Study of $[\text{KC}_8]\text{PF}_6$. The box adopts a structure typical for $\text{M}_8(\text{CN})_{12}$ cages. The cyanide ligands are ordered, as revealed by the CpCo–C distances being on average 0.096 Å shorter than the Cb*Co–N distances. Further evidence that the cyanide ligands remain ordered is provided by the greater linearity of the average Co–C≡N angle (174.6°) versus the average Co–N≡C angle (168.2°) (see Table 1 and Figure

(17) Holmes, S. M.; Girolami, G. S. *J. Am. Chem. Soc.* **1999**, *121*, 5593–5594.
 (18) (a) Boulas, P. L.; Gomezkaifer, M.; Echegoyen, L. *Angew. Chem., Int. Ed.* **1998**, *37*, 216–247. (b) Kaifer, A. E. *Acc. Chem. Res.* **1999**, *32*, 62–71.
 (c) Tucker, J. H. R.; Collinson, S. R. *Chem. Soc. Rev.* **2002**, *31*, 147–156.
 (d) Beer, P. D.; Gale, P. A.; Chen, G. Z. *J. Chem. Soc., Dalton Trans.* **1999**, 1897–1910.
 (19) Plenio, H.; Aberle, C. *Organometallics* **1997**, *16*, 5950–5957.
 (20) Webber, P. R. A.; Beer, P. D.; Chen, G. Z.; Felix, V.; Drew, M. G. B. *J. Am. Chem. Soc.* **2003**, *125*, 5774–5785.

(21) Butovskii, M. V.; Englert, U.; Fil'chikov, A. A.; Herberich, G. E.; Koelle, U.; Kudinov, A. R. *Eur. J. Inorg. Chem.* **2002**, 2656–2663.

Scheme 2. Ion Exchange in [MCo₈]⁺ Cages

1). The cyanide linkers deviating from linearity have been previously reported.^{5,7,8,22} Distortion from T_d symmetry is due in part to the C–Co–C and N–Co–N angles, which range from 84.15 to 93.11° and 90.35 to 95.85°, respectively. Considering Cb* as a bidentate ligand, one might expect that the N–Co–(I)–N angles would be significantly greater than 90°, but they are 90.35, 90.36, and 95.35°. For each [CpCo(CN)₃][−] subunit, two cyanide groups form short contacts and one forms a longer contact with the encapsulated cation. Thus, eight Co–CN–Co edges of the cube bow inward toward the encapsulated K⁺, and the remaining four μ -CN ligands bow outward. The four edges that bow outward display K–C and K–N distances of 3.841(34) and 3.893(39) Å, respectively, whereas the remaining eight edges of the cube display shorter K–C distances of 3.5326(34) and 3.4555(34) Å and K–N distances of 3.3827(29) and 3.3035(28) Å. The distortion of the [KCo₈]⁺ cage due to nonlinearity of the cyanide bridges can be compared to other potassium-containing cages such as (NEt₄)₃{K[Cp*Rh(CN)₃]₄(CO)₃Mo₄}.¹¹ In this cubic cage the average Rh–C≡N angle is 177.34° and the average Mo–N≡C angle is 173.29°.

Ion-Exchange Properties of Co₈ Boxes. MeCN solutions of [KCo₈]⁺ were found to react readily with Cs⁺ to give [CsCo₈]⁺ (Scheme 2). The ¹³³Cs NMR spectrum of [CsCo₈]⁺ exhibits a singlet at δ 0.12, which is consistent with binding of Cs⁺ at the interior of a cyanometalate box.¹¹ ¹H NMR spectra do not clearly distinguish binding of Cs⁺ versus K⁺: for Cb* $\Delta\delta$ is 0.006 and for Cp $\Delta\delta$ = 0.008 ppm. ESI-MS confirmed the presence of [CsCo₈]⁺ (m/z = 1609 amu). No signal was observed for the [KCo₈]⁺ starting material. The [CsRh₄Co₄]⁺ analogue was prepared similarly from [KRh₄Co₄]⁺ and CsOTf. ESI-MS confirmed the presence of [CsRh₄Co₄]⁺ (m/z = 2065) with no peak corresponding to [KRh₄Co₄]⁺ observed.

[CsCo₈]⁺ could also be efficiently generated by the Cs⁺-templated reaction of PPN[CpCo(CN)₃] and [Cb*Co(NCMe)₃]-PF₆. When this same reaction was conducted with a deficiency of [Cb*Co(NCMe)₃]-PF₆, ESI-MS indicated that [CsCo₈]⁺ was the major product; peaks corresponding to seven-vertex cages,^{9,23} such as Cs[CpCo(CN)₃]₄[Cb*Co]₃, were not observed.

Labeling experiments demonstrated that Cs⁺-for-K⁺ ion exchange proceeds via significant fragmentation of the cage

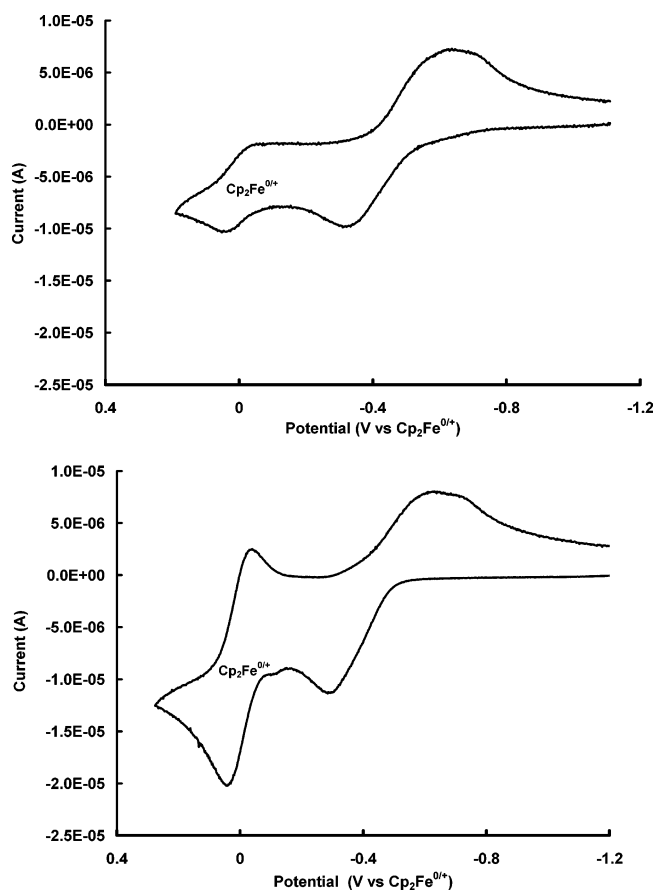


Figure 2. Cyclic voltammograms of [KCo₈]⁺ (top) and [CsCo₈]⁺ (bottom) at scan rates of 0.2 V/s in a 0.1 M NBu₄PF₆/MeCN solution.

followed by reassembly (Scheme 2). The robustness of the MCo₈ cages was first established by examining the quasi-degenerate reaction involving MeCN solutions of [KCo₈]⁺ and K[Cp'Co(CN)₃] (Cp' = MeC₅H₄): after 5 h at room temperature, <5% of {K[CpCo(CN)₃]₃[Cp'Co(CN)₃]₁[Cb*Co]₄}⁺ was observed by ESI-MS. A similar absence of vertex exchange was found to occur in solutions of [CsCo₈]⁺ and K[Cp'Co(CN)₃]. Under otherwise analogous conditions, treatment of a MeCN solution of [KCo₈]⁺PF₆ with 4 equiv each of [Cp'Co(CN)₃][−] and CsOTf induced rapid vertex exchange, affording {Cs[CpCo(CN)₃]_{4-x}[Cp'Co(CN)₃]_x[Cb*Co]₄}⁺PF₆, with the following product ratio of 1 ($x = 0$):0.7 ($x = 1$):0.3 ($x = 2$):0.26 ($x = 3$). This result suggests that ion exchange induces vertex exchange. The preceding experiments led us to re-examine the reaction of {[CpCo(CN)₃]₄[Cp*Ru]₄} with CsOTf in the presence of K[Cp'Co(CN)₃]: no vertex exchange was detected, consistent with previous claims.¹²

The behavior of the ammonium-containing box was also consistent with the kinetic lability of these Cb*Co-based cages. Ion exchange of NH₄⁺ with [KCo₈]⁺ proceeds to completion in THF solution. In MeCN solution, however, attempted ion exchange afforded [Cb*Co(NCMe)₃]-PF₆ and the poorly soluble salt NH₄[CpCo(CN)₃]. Even MeCN solutions of preformed [NH₄Co₈] cage deposited uncharacterized solids over the course of 12 h. The enhanced lability of the [NH₄Co₈]⁺ was further confirmed by the rapid exchange of the acidic protons in [NH₄Co₈]⁺ with D₂O–CD₃CN. The lability of the [NH₄Co₈]⁺ cage differs from that of the previously reported {[NH₄]₄[CpCo(CN)₃]₄[Cp*Ru]₄}⁺ cage that was unaffected by D₂O.¹²

(22) Richardson, G. N.; Brand, U.; Vahrenkamp, H. *Inorg. Chem.* **1999**, *38*, 3070–3079.

(23) Kuhlman, M. L.; Rauchfuss, T. B. *J. Am. Chem. Soc.* **2003**, *125*, 10084–10092.

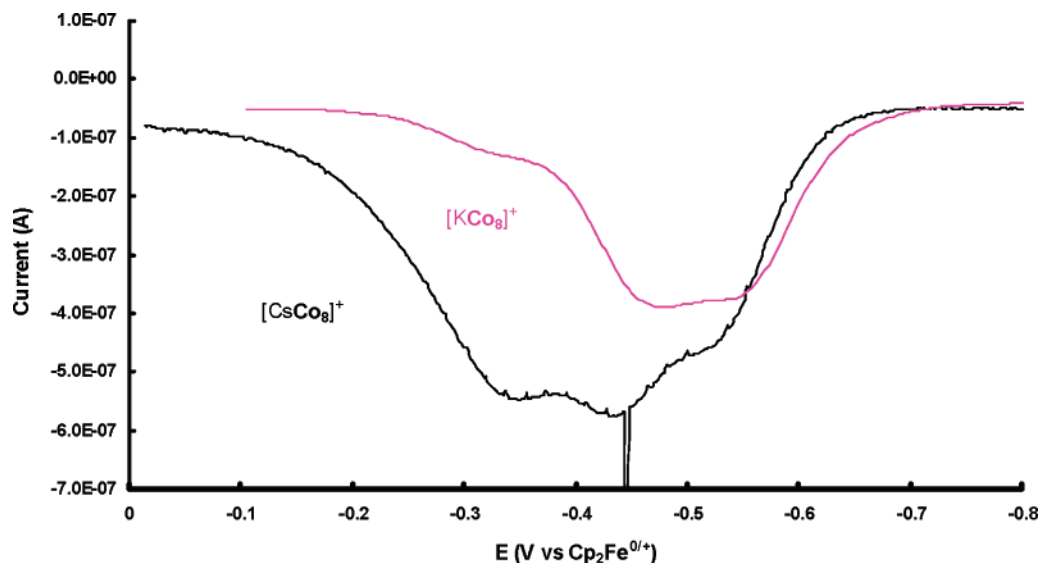


Figure 3. DPV of $[\text{KCo}_8]^+$ (pink) and $[\text{CsCo}_8]^+$ (black) at scan rates of 10 mV/s in a 0.1 M $\text{NEt}_4\text{BARF}_4/\text{CH}_2\text{ClCH}_2\text{Cl}$ solution.

Oxidation of $[\text{MCo}_8]^+$. Treatment of a purple MeCN solution of $[\text{MCo}_8]^+$ with 4 equiv of FcPF_6 produced the orange species $[\text{Co}_8]^{4+}$. The ^{133}Cs NMR spectrum of the resulting solution verified the formation of $[\text{Cs}(\text{NCMe})_n]^+$, confirming that oxidation expelled the cation from the cage. The formation of the empty tetracationic $[\text{Co}_8]^{4+}$ cage was indicated for both $[\text{KCo}_8]^+$ and $[\text{CsCo}_8]^+$.

The $[\text{Co}_8](\text{PF}_6)_4$ salt was further characterized by the Evans ^1H NMR method. The susceptibility varied linearly versus $1/T$ over the temperature range of 253–343 K. This behavior is described by Curie–Weiss Law and is consistent with the presence of four low-spin d^7 centers per cage, that is, $[\text{Co}^{\text{III}}_4\text{Co}^{\text{II}}_4]^{4+}$. The IR spectrum of this salt featured a ν_{CN} band at 2159 versus 2146 cm^{-1} for $[\text{KCo}_8]^+$ in MeCN solution, indicating a stronger N–Co bonds after oxidation of the Cb^*Co subunit.

The oxidation-induced dissociation of Cs^+ from $[\text{CsCo}_8]^+$ is chemically reversible. Treatment of a solution equimolar in $[\text{Co}_8]^{4+}$ and CsOTf with 4 equiv of Cp_2Co yielded $[\text{CsCo}_8]^+$ in good yield, as confirmed by ^1H NMR spectroscopy and ESI-MS. In the absence of CsOTf , reduction of $[\text{Co}_8]^{4+}$ with 4 equiv of Cp_2Co gave an insoluble solid, illustrating the importance of the alkali metal cation in stabilization of the cage.

Electrochemical Studies. Cation recognition by $[\text{Co}_8]$ and $[\text{Rh}_4\text{Co}_4]$ cages was investigated electrochemically using cyclic voltammetry and differential pulse voltammetry (DPV). At scan rates of 0.05 V/s, all compounds exhibited a single broad redox wave with a half-cell potential of -0.51 to -0.42 V versus $\text{Cp}_2\text{Fe}^{0/+}$. Each of the compounds exhibited a single oxidation wave of apparent multielectron height. As shown in Figure 2, the cage's redox wave was broader than that of the ferrocene standard and was coupled to a broad reverse cathodic wave. The general shapes of these redox waves in Figure 2 are consistent with multielectron, chemically reversible, redox processes. Bulk electrolysis of a MeCN solution of $[\text{KCo}_8]^+$ at $E_{\text{appl}} = 0.4$ V confirmed the four-electron stoichiometry of the anodic process. Studies are underway to examine the details of these non-Nernstian redox processes.²⁴

(24) Electrochemical work is being carried out in collaboration with D. Chong and W. Geiger, University of Vermont. It is particularly interesting that there are significant medium effects, including a shift to an overall two-electron stoichiometry in a dichloroethane/ $[\text{NBu}_4][\text{B}(\text{C}_6\text{F}_5)_4]$ electrolyte.

Table 2. Electrochemical Data for Scan Rates of 0.2 V/s in 0.1 M NBu_4PF_6 in MeCN Solution

compound	$E_{1/2}$ (V vs Cp_2Fe)
$[\text{KCo}_8]^+$	−0.50
$[\text{CsCo}_8]^+$	−0.42
$[\text{KRh}_4\text{Co}_4]^+$	−0.51
$[\text{CsRh}_4\text{Co}_4]^+$	−0.46

The values of $E_{1/2}$ for the boxes differed for the Cs^+ versus K^+ derivatives (Table 2). The potassium-containing $[\text{KCo}_8]^+$ cage was more easily oxidized (-0.51 V vs $\text{Cp}_2\text{Fe}^{0/+}$) than $[\text{CsCo}_8]^+$ (-0.42 V). The difference in $E_{1/2}$ for the heterometallic $[\text{CsRh}_4\text{Co}_4]^+$ cage and $[\text{KRh}_4\text{Co}_4]^+$ was smaller at 50 mV. The $\Delta E_{1/2}$ for the $[\text{KCo}_8]^+$ vs $[\text{CsCo}_8]^+$ can be further amplified using non-polar solvents and larger, less coordinating electrolytes. The differential pulse voltammetry (DPV) of dichloroethane solutions with $\text{NEt}_4[\text{BARF}_4]$ ($\text{BARF}_4 = \text{B}(\text{C}_6\text{H}_3-3,5-(\text{CF}_3)_2)_4$) electrolyte displayed a 180 mV difference between $[\text{KCo}_8]^+$ (-0.69 V vs. Cp_2Fe) and $[\text{CsCo}_8]^+$ (-0.51 V, vs. Cp_2Fe). The DPV of $[\text{CsCo}_8]^+$ (Figure 3) also clearly shows the emergence of overlapping oxidation peaks, further suggesting a coupled multielectron oxidation.

Summary and Conclusions

The present report describes a new family of organo-cyanometalate cages that are based on the Cb^*Co^+ vertex (Scheme 2). The new cages are ionophilic as we have come to expect when the framework is neutral or anionic.^{7–9} Indeed, we were unable to generate charge-neutral Cb^*Co -containing boxes; only the cation-templated routes successfully afforded molecular cages.

The alkali metal adducts are robust, although we showed that ion exchange occurs via disassembly of the cage. A crystallographic study revealed that the K^+ -containing Co_8 box is highly distorted, which may be relevant to the lability of the vertices. Previous work showed that related $\{[\text{CpCo}(\text{CN})_3]_4-[\text{Cp}^*\text{Ru}]_4\}$ cages are kinetically inert, even upon ion exchange.¹² The differing kinetic labilities of the presently described $[\text{Cb}^*\text{Co}]^+$ cages versus those containing $[\text{Cp}^*\text{Ru}]^+$ vertices probably reflect the diminished strengths of $\text{Co}(\text{I})-\text{N}$ versus

Ru(II)–N bonds. The pathway by which Cs⁺ causes the scission of the Cb*Co–NCCoCp bonds in [KC₈O₈]⁺ is not known, although it is reasonable to propose that the first step entails binding of Cs⁺ to a Co₄(μ-CN)₄ face.²⁵

Upon oxidation at mild potentials, the cages release the alkali metal guest. The reversibility of this process was verified with preparative-scale redox interconversions. The Co₈ and Rh₄Co₄ cages “recognize” the cations in the sense that the encapsulated cations have distinguishable redox properties, but the multi-electron nature of the redox conversions gives rise to broad redox waves, obscuring differences in redox couples. One obvious approach for simplifying the redox properties of the K⁺-versus-Cs⁺-derived cages would entail the preparation of boxes with only one redox center, and efforts along these lines are planned.

Experimental Section

Operations were performed under a nitrogen atmosphere as described in previous papers by this group unless otherwise noted.²⁶ [Cb*Co(NCMe)₃]₃PF₆,²¹ K[CpCo(CN)₃],²⁷ and (MeC₅H₄)Co(CO)₂²⁸ were prepared according to literature methods. ¹³³Cs NMR spectra were recorded with a Varian Unity Inova 600 MHz spectrometer, and the chemical shift of CD₃CN solution of CsOTf was referenced at δ 34.32. Electrospray ionization-mass spectra (ESI-MS) and MS–MS measurements were acquired using a Micromass Quattro QHQ quadrupole–hexapole–quadrupole instrument.

Electrochemistry. The cyclic voltammetry experiments were conducted in a ~10 mL one- or three-compartment glass cell. The counter electrode was a Pt wire; the reference electrode was Ag/AgCl, and the working electrode was glassy carbon (2 mm diameter). All potentials reported in this paper are given versus the ferrocene/ferrocenium couple.²⁹ Electrochemistry experiments were performed in drybox under nitrogen atmosphere and employed a PARC model 273 potentiostat/galvanostat interfaced to a personal computer. Electrochemistry experiments were performed in an inert atmosphere at concentrations ~0.4 mM in MeCN/1.0 mM NBu₄PF₆. Controlled potential electrolysis was performed at a Pt basket working electrode in a three-compartment cell. Spectro-grade MeCN was distilled under nitrogen from CaH₂, followed by freeze–pump–thaw cycles before electrochemical experiments.

{K[CpCo(CN)₃]₄[Cb*Co]₄}(PF₆)₄, [KC₈O₈](PF₆)₄. A solution of 870 mg (2 mmol) of [Cb*Co(NCMe)₃]₃PF₆ in 40 mL of MeCN was added dropwise to a stirred solution of 482 mg (2 mmol) of K[CpCo(CN)₃] in 160 mL of MeCN. The resulting dark purple solution was stirred for 4 h, and then the solvent was removed under vacuum. The residue was extracted with 3 × 15 mL of 1:1 Et₂O–CH₂Cl₂. Evaporation of solvent left a dark purple solid, which was crystallized by extraction into 15 mL of MeCN diluted with 150 mL of Et₂O. Yield: 620 mg (75%). ¹H NMR (CD₃CN): δ 5.580 (s, 20H), 0.964 (s, 48H). ESI-MS (*m/z*): 1515 ([KCb*₄Cp₄Co₈(CN)₁₂]⁺). IR (MeCN, cm⁻¹): ν_{CN} = 2147. Anal. Calcd for C₆₄H₆₈Co₈F₆KN₁₂P (found): C, 46.28 (46.22); H, 4.13 (4.05); N, 10.12 (10.26).

{Cs[CpCo(CN)₃]₄[Cb*Co]₄}(PF₆)₄, [CsC₈O₈](PF₆)₄. A solution of 166 mg (0.1 mmol) of {K[CpCo(CN)₃]₄[Cb*Co]₄}(PF₆)₄ and 42 mg (0.15 mmol) of CsOTf in 10 mL of MeCN was stirred for 1 h, and then the solvent volume was reduced to 2 mL under vacuum. To this concentrated solution was added 30 mL of degassed H₂O. The dark red precipitate was collected by filtration. The product was extracted with two 5 mL portions of CH₂Cl₂. The crude product was dissolved

in MeCN and precipitated upon addition of Et₂O. Yield: 145 mg (83%). ¹H NMR (CD₃CN): δ 0.96 (s, 48H), 5.59 (s, 20H). ¹³³Cs NMR (CD₃CN): δ 0.11. ESI-MS (*m/z*): 1609 ([CsCb*₄Cp₄Co₈(CN)₁₂]⁺). Anal. Calcd for C₆₄H₆₈Co₈CsF₆N₁₂P (found): C, 43.81 (44.69); H, 3.91 (3.91); N, 9.58 (9.14).

{NH₄[CpCo(CN)₃]₄[Cb*Co]₄}(PF₆)₄, [NH₄C₈O₈](PF₆)₄. A solution of 100 mg (0.06 mmol) of [KC₈O₈](PF₆)₄ and 15 mg (0.09 mmol) of NH₄PF₆ in 10 mL of THF was stirred for 3 h. After evaporation of the solvent, the product was extracted from the residue with two 5 mL portions of CH₂Cl₂. The CH₂Cl₂ extract was concentrated to 2 mL and then diluted with 10 mL of Et₂O and 6 mL of hexane to precipitate the product as a dark red solid, which was collected by filtration and dried under vacuum. Yield: 59 mg (60%). ¹H NMR (CD₃CN): δ 5.58 (s, 20H), 3.76 (t, 4H), 0.97 (s, 48H). ESI-MS (*m/z*): 1494 ([NH₄Cb*₄Cp₄Co₈(CN)₁₂]⁺). Anal. Calcd for C₆₄H₇₂Co₈F₆N₁₃P·(CH₂Cl₂)₄ (found): C, 41.24 (41.94); H, 4.08 (3.13); N, 9.20 (9.30).

{[CpCo(CN)₃]₄[Cb*Co]₄}(PF₆)₄, [Co₈](PF₆)₄. A solution of 80 mg (0.24 mmol) of [Cp₂Fe]PF₆ in 12 mL of MeCN was added dropwise to a stirred solution of 100 mg (0.06 mmol) of {K[C₈O₈]}PF₆ in 12 mL of MeCN at 0 °C. The resulting orange solution was stirred for 10 h at room temperature, before the solvent volume was reduced to ~2 mL under vacuum. Addition of 30 mL of THF precipitated an orange-colored product, which was collected by filtration and washed with 10 mL of THF. Yield: 72 mg (58%). ESI-MS (*m/z*): 369 ([Cb*₄Cp₄Co₈(CN)₁₂]⁴⁺). IR (MeCN, cm⁻¹): ν_{CN} = 2159. Anal. Calcd for C₆₄H₆₈Co₈F₂₄N₁₂P₄ (found): C, 37.38 (37.41); H, 3.33 (3.25); N, 8.17 (7.95). The magnetic moment was determined using a solution of [Co₈](PF₆)₄ (6.9 mg, 0.0034 mmol) in 0.7 mL of a stock solution of CD₃CN containing a trace of C₆D₆. The ¹H NMR spectrum was recorded from –20 to 70 °C.

(MeC₅H₄)CoI₂(CO). A solution of 7.1 g (27 mmol) of I₂ in 60 mL of MeOH was added to a stirred solution of 5.2 g (27 mmol) of (MeC₅H₄)Co(CO)₂ in 80 mL of MeOH at 0 °C. After stirring the reaction mixture at room temperature for 3 h, the solvent was evaporated. The dark red solid was washed with 200 mL of hexane and then extracted into CH₂Cl₂. This extract was passed through a 3 cm column of silica gel and washed with CH₂Cl₂. The resulting crude product was purified by chromatography on a 15 × 2 cm column of silica gel, eluting with 50% hexane–CH₂Cl₂. Evaporation of the intense red band afforded a dark red solid. Yield: 8.1 g (72%). ¹H NMR (CD₃COCD₃): δ 5.81 (t, 2H, *J* = 2 Hz, C₅H₄), 5.70 (t, 2H, *J* = 2 Hz, C₅H₄), 2.48 (s, 3H, CH₃). IR (KBr, cm⁻¹): ν_{CO} = 2052. EI (*m/z*): 419.8. Anal. Calcd for C₇H₇CoI₂O (found): C, 20.02 (20.01); H, 1.68 (1.72).

K{[CpCo(CN)₃]₄[Cb*Co]₄}. A slurry of 8.4 g (20 mmol) of (MeC₅H₄)Co(CO)I₂ in 100 mL of MeOH was added to a stirred solution of 4.1 g (63 mmol) of KCN in 100 mL of MeOH. The reaction mixture was heated at reflux for 60 h and then allowed to cool before filtering in air. The brown-colored filtrate was evaporated to dryness to give crude product. This residue was extracted with 30 mL of MeCN, which upon cooling to –20 °C overnight gave 3.1 g of pure orange crystals. A second extraction using 3 × 100 mL of MeCN gave an orange–yellow solution, which was evaporated to dryness. After washing the residue with 40 mL of Me₂CO to remove a dark brown impurity, the remaining product was then extracted with 150 mL of MeCN. Evaporation of the MeCN extract gave a further crop of 1.9 g. The combined products were dried under vacuum at 80 °C for 24 h. Yield: 4.3 g (84%). ¹H NMR (CD₃CN): δ 5.10 (t, 2H, *J* = 2 Hz, C₅H₄), 5.04 (t, 2H, *J* = 2 Hz, C₅H₄), 2.21 (s, 2H, H₂O), 1.89 (s, 3H, CH₃). IR (KBr, cm⁻¹): ν_{CN} = 2132, 2116, 2113. ESI-MS (*m/z*): 216 ([C₉H₇CoN₃]⁺). Anal. Calcd for C₉H₇CoKN₃ (found): C, 42.36 (40.80); H, 2.77 (2.71); N, 16.47 (15.54).

{K[Cp*Rh(CN)₃]₄[Cb*Co]₄}(PF₆)₄, [KRh₄Co₄](PF₆)₄. This compound was prepared from KCp*Rh(CN)₃ (373 mg, 1 mmol) by a procedure analogous to the preparation of [KC₈O₈](PF₆)₄. The product was isolated as a red powder. Yield: 453 mg (86%). ¹H NMR (CD₃CN): δ 2.04 (s, 60H), 0.91 (s, 48 H). ESI-MS (*m/z*): 1971 ([KCb*₄Cp*₄Rh₄Co₄(CN)₁₂]⁺).

(25) Ramesh, M.; Rauchfuss, T. B. *J. Organomet. Chem.* **2004**, 689, 1425–1430.

(26) Schwarz, D. E.; Rauchfuss, T. B.; Wilson, S. R. *Inorg. Chem.* **2003**, 42, 2410–2417.

(27) Contakes, S. M.; Klausmeyer, K. K.; Rauchfuss, T. B. *Inorg. Synth.* **2004**, 34, 166–171.

(28) Rausch, M. D.; Genetti, R. A. *J. Org. Chem.* **1970**, 35, 3888–3897.

(29) Connelly, N. G.; Geiger, W. E. *Chem. Rev.* **1996**, 96, 877–910.

IR (KBr, cm^{-1}): $\nu_{\text{CN}} = 2146$. Anal. Calcd for $\text{C}_{84}\text{H}_{108}\text{Co}_4\text{F}_6\text{KN}_{12}\text{PRh}_4$ (found): C, 47.63 (46.17); H, 5.14 (4.99); N, 7.94 (7.50).

$\{\text{Cs}[\text{Cp}^*\text{Rh}(\text{CN})_3]_4[\text{Cb}^*\text{Co}]_4\}\text{PF}_6$, $[\text{CsRh}_4\text{Co}_4]\text{PF}_6$. This compound was prepared from 148 mg (0.07 mmol) of $\{\text{K}[\text{Cp}^*\text{Rh}(\text{CN})_3]_4[\text{Cb}^*\text{Co}]_4\}\text{PF}_6$ via ion exchange in a procedure analogous to the preparation of $[\text{CsCo}_8]\text{PF}_6$. The product was isolated as red powder. Yield: 58 mg (43%). ^1H NMR (CD_3CN): δ 2.04 (s, 60H), 0.91 (s, 48 H). ESI-MS (m/z): 2065 ($[\text{CsCb}^*_4\text{Cp}^*_4\text{Rh}_4\text{Co}_4(\text{CN})_{12}]^+$). IR (KBr, cm^{-1}): $\nu_{\text{CN}} = 2148$.

Labeling Experiment on Vertex Exchange in $[\text{KCo}_8]^+ + \text{Cs}^+$ and Control Experiments. A solution of 11 mg (0.04 mmol) of $\text{K}[(\text{MeC}_5\text{H}_4)\text{Co}(\text{CN})_3]$, 17 mg (0.01 mmol) of $[\text{KCo}_8]\text{PF}_6$, and 4 mg (0.015 mmol) of CsOTf in 5 mL of MeCN was stirred for 5 h. A 0.1 mL sample of reaction mixture was diluted with 2 mL of MeCN. ESI-MS (m/z): 1609 ($[\text{CsCb}^*_4\text{Cp}_4\text{Co}_8(\text{CN})_{12}]^+$, 100%), 1623 ($[\text{CsCb}^*_4\text{Cp}_3(\text{MeC}_5\text{H}_4)\text{Co}_8(\text{CN})_{12}]^+$, 70%), 1637 ($[\text{CsCb}^*_4\text{Cp}_2(\text{MeC}_5\text{H}_4)_2\text{Co}_8(\text{CN})_{12}]^+$, 34%), 1651 ($[\text{CsCb}^*_4\text{Cp}(\text{MeC}_5\text{H}_4)_3\text{Co}_8(\text{CN})_{12}]^+$, 25%).

Control Experiments: (1) Reaction of $[\text{KCo}_8]\text{PF}_6$ and $\text{K}[(\text{MeC}_5\text{H}_4)\text{Co}(\text{CN})_3]$. A solution of 11 mg (0.04 mmol) of $\text{K}[(\text{MeC}_5\text{H}_4)\text{Co}(\text{CN})_3]$ and 17 mg (0.01 mmol) of $[\text{KCo}_8]\text{PF}_6$ in 5 mL of MeCN was stirred for 5 h. A 0.1 mL sample of reaction mixture was diluted with 2 mL of MeCN and analyzed by ESI-MS. ESI-MS (m/z): 1515 ($[\text{KCb}^*_4\text{Cp}_4\text{Co}_8(\text{CN})_{12}]^+$, 100%), 1529 ($[\text{KCb}^*_4\text{Cp}_3(\text{MeC}_5\text{H}_4)\text{Co}_8(\text{CN})_{12}]^+$, 4%). **(2) Reaction of $[\text{CsCo}_8]\text{PF}_6$ and $\text{K}[(\text{MeC}_5\text{H}_4)\text{Co}(\text{CN})_3]$.** A solution of 11 mg (0.04 mmol) of $\text{K}[(\text{MeC}_5\text{H}_4)\text{Co}(\text{CN})_3]$ and 18 mg (0.01 mmol) of $[\text{CsCo}_8]\text{PF}_6$ in 5 mL of MeCN was stirred for 5 h. A 0.1 mL sample of reaction mixture was diluted with 2 mL of MeCN and analyzed by ESI-MS. ESI-MS (m/z): 1609 ($[\text{CsCb}^*_4\text{Cp}_4\text{Co}_8(\text{CN})_{12}]^+$, 100%), 1623 ($[\text{CsCb}^*_4\text{Cp}_3(\text{MeC}_5\text{H}_4)\text{Co}_8(\text{CN})_{12}]^+$, 5%). **(3) Reaction of $[\text{CpCo}(\text{CN})_3(\text{Cp}^*\text{Ru})_4]$, $\text{K}[(\text{MeC}_5\text{H}_4)\text{Co}(\text{CN})_3]$, and CsOTf .** A solution of 11 mg (0.04 mmol) of $\text{K}[(\text{MeC}_5\text{H}_4)\text{Co}(\text{CN})_3]$, 18 mg (0.01 mmol) of $[\text{CpCo}(\text{CN})_3(\text{Cp}^*\text{Ru})_4]$, and 4 mg (0.015 mmol) of CsOTf in 5 mL of MeCN was stirred for 5 h. A 0.1 mL sample of the purple reaction mixture was removed and diluted with 2 mL of MeCN, which was analyzed by ESI-MS (m/z): 1793 ($[\text{KCp}_4\text{Cp}^*_4\text{Co}_4\text{Ru}_4]^+$, 100%).

Crystallography. Crystals were mounted to a thin glass fiber using Paratone-N oil (Exxon). Data were filtered to remove statistical outliers. The integration software (SAINT) was used to test for crystal decay as a bilinear function of X-ray exposure time and sine (θ). Data were collected at Siemens Platform/CCD automated diffractometer. Crystal and refinement details are given in Table 3. The structures were solved using SHELXTL by direct methods;³⁰ correct atomic positions were deduced from an E map or by an unweighted difference Fourier synthesis. H atom U 's were assigned as 1.2 times the U_{eq} 's of adjacent

Table 3. Crystallographic Data for $[\text{KCo}_8]\text{PF}_6 \cdot \text{THF}^a$

empirical formula	$\text{C}_{72}\text{H}_{84}\text{Co}_8\text{F}_6\text{KN}_{12}\text{O}_2\text{P}$
formula weight	1805.02
temperature	193(2) K
wavelength	0.71073 Å
crystal system	tetragonal
space group	$P4_2/c$
a (Å)	12.853(4)
b (Å)	12.853(4)
c (Å)	23.193(14)
α (deg)	90.00
β (deg)	90.00
γ (deg)	90.00
V (Å ³)	3832(3)
Z	2
density (calculated)	1.565 mg/m^3
absorption coefficient	1.829 mm^{-1}
crystal size	$0.16 \times 0.16 \times 0.07$ mm
θ range for data collection	$2.85\text{--}25.45^\circ$
index ranges	$-15 \leq h \leq 15, -15 \leq k \leq 15, -28 \leq l \leq 27$
reflections collected/unique	30511/3525 [$R_{\text{int}} = 0.0906$]
absorption correction	integration
max. and min. transmission	0.8820 and 0.7630
refinement	full-matrix least-squares on F^2
data/restraints/parameters	3525/45/257
goodness-of-fit on F^2	1.013
final R indices (obsd data)	$R1 = 0.0332, wR2 = 0.0618$
R indices (all data)	$R1 = 0.0469, wR2 = 0.0656$
largest diff. peak and hole	0.342 and $-0.263 \text{ e} \cdot \text{Å}^{-3}$

$$^a R1 = \sum ||F_o| - |F_c|| / \sum |F_o|, wR2 = \{ \sum [w(F_o^2 - F_c^2)^2] / \sum [w(F_o^2)^2] \}^{1/2}.$$

C atoms. Non-H atoms were refined with anisotropic thermal coefficients. Successful convergence of the full-matrix least-squares refinement of F^2 was indicated by the maximum shift/error for the last cycle.³¹

Acknowledgment. This research was supported by the U.S. Department of Energy (UIUC). We thank Professor W. E. Geiger for advice and collaboration on preliminary measurements, and D. Chong for advice and help with the electrochemical measurements.

Supporting Information Available: Crystallographic details for $\{\text{K}[\text{CpCo}(\text{CN})_3]_4[\text{Cb}^*\text{Co}]_4\}\text{PF}_6$. Curie–Weiss plot for $\{[\text{CpCo}(\text{CN})_3]_4[\text{Cb}^*\text{Co}]_4\}(\text{PF}_6)_4$. This material is available free of charge via the Internet at <http://pubs.acs.org>.

JA0646545

(30) Scheldrick, G. M. *SHELXTL*; University of Göttingen: Göttingen, Germany, 1997.

(31) The supplementary crystallographic data for $\{\text{K}[\text{CpCo}(\text{CN})_3]_4[\text{Cb}^*\text{Co}]_4\}\text{PF}_6$ (CCDC-633957) can be obtained free of charge from the Cambridge Crystallographic Data Centre at www.ccdc.cam.ac.uk/data_request/cif.